

Note: Updates to an ultra-low noise laser current driver

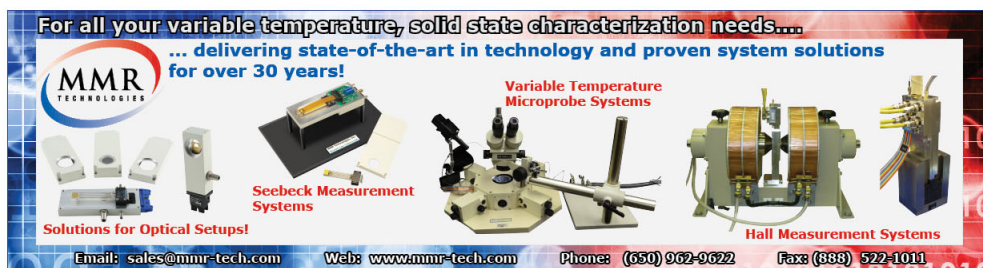
Daylin L. Troxel, Christopher J. Erickson, and Dallin S. Durfee

Citation: [Review of Scientific Instruments](#) **82**, 096101 (2011); doi: 10.1063/1.3630950

View online: <http://dx.doi.org/10.1063/1.3630950>

View Table of Contents: <http://scitation.aip.org/content/aip/journal/rsi/82/9?ver=pdfcov>

Published by the [AIP Publishing](#)



For all your variable temperature, solid state characterization needs....
... delivering state-of-the-art in technology and proven system solutions
for over 30 years!

MMR TECHNOLOGIES

Seebeck Measurement Systems

Variable Temperature Microprobe Systems

Hall Measurement Systems

Solutions for Optical Setups!

Email: sales@mmr-tech.com Web: www.mmr-tech.com Phone: (650) 962-9622 Fax: (888) 522-1011

Note: Updates to an ultra-low noise laser current driver

Daylin L. Troxel, Christopher J. Erickson, and Dallin S. Durfee^{a)}

BYU Department of Physics and Astronomy and Brigham Young University, Provo, Utah 84602, USA

(Received 25 May 2011; accepted 9 August 2011; published online 1 September 2011)

We describe updates to our current driver design allowing for higher output currents, both positive and negative currents, and updated digital interfacing to the microcontroller. We also discuss measurement of the noise spectral density of the driver with a better technique, showing that the driver's actual current noise density is about an order of magnitude lower than the upper limit we previously determined. © 2011 American Institute of Physics. [doi:10.1063/1.3630950]

In many diode laser applications the phase, wavelength, or amplitude of the light has to be controlled very precisely, requiring a precision low-noise and low-drift current driver. In Ref. 1 we presented a laser current driver design improving upon the Hall-Libbrecht model.² This driver exhibits lower noise and drift than any other driver we are aware of, as well as high modulation bandwidth and excellent repeatability using digital set-point control.

This Note describes modifications to the original design which increases the versatility of the driver. We also present new data on the noise characteristics of the driver using a measurement technique with a much lower noise floor than in Ref. 1.

A detailed description of the current driver's operation is given in Ref. 1. We recently modified the design to create a single printed circuit board (PCB) which could produce either positive or negative current with a maximum current capacity ranging from milli-amperes up to several amperes by changing a few components. We also modified the digital interface to minimize crosstalk and allow control of several devices (i.e., a current driver with a temperature controller and a PID lock circuit) with one microcontroller. Figure 1 highlights the most significant changes. An annotated full schematic and PCB layout can be found in Ref. 3.

In the updated design, a positive supply can be realized by connecting jumpers whose labels begin with “Jp” or “J+” in Fig. 1. A negative supply can be constructed from the same PCB by connecting jumpers beginning with “Jn” or “J-.” For positive/negative supplies we use an LM317/LM337 as the principal voltage regulator. The PCB provides separate pads for each, but only one should be installed at a time. For a negative supply all of the diodes must be reversed in polarity from the positive supply configuration shown in Fig. 1. For the transistor Q_{en} we use an MMBT2097A/MMBT2222A for a positive/negative supply. Both transistors use the same pads.

For applications requiring up to ± 1 A, the LM317/LM337 can be used in an SOT-223 package. In a TO-220 package they can source up to 1.5 A. An LM388 can source up to +5 A. We were unable to find a high-current regulator similar to the LM337, so for high-current negative applications we spliced in an off-board high-current transistor follower after an LM337 voltage regulator. With higher

current regulators it is important to make sure heat sink requirements are met, and it may be necessary to reduce the value of R_{filt} . Through holes are provided on the PCB for installing a leaded power resistor if necessary.

We added through-hole pads in addition to the surface mount pads for the current sense resistor R_s . This allows the use of precision, low temperature coefficient resistors for lower current supplies, or power resistors for high-current drivers. The PCB accommodates current regulating MOSFETs in either an SOT-23 or a TO-220 package for low- and high-current supplies. The same pads and through holes can be used for both P- and N-type MOSFETs. For positive current sources we use an NDS0605 for supplies up to 180 mA, and an IRF9Z14 for sources up to 6.7 A. We use an NDS7002A for low current negative supplies or an IRF510 for negative currents up to 5.6 A. Proper heat sinking is necessary for the higher current chips.

We found that with higher current MOSFETs the 8.5 nF capacitor and 10 k Ω resistor shown in Fig. 1 of Ref. 1 needed to be adjusted to prevent oscillation. A rule of thumb is to scale the capacitor with the gate capacitance of the MOSFET. For example, the IRF9Z14 has a gate capacitance roughly 3.4 times the capacitance of the NDS0605, and can be stabilized by a 33 nF capacitor and a 10 k Ω resistor. When using the IRF510, capacitance scaling was not enough, and we ended up using a 1 μ F capacitor with a 100 k Ω resistor.

The output of the driver is equal to $(V_{reg} - V_{set})/R_s$, where V_{reg} is the voltage generated in the voltage regulation circuit, R_s is the resistance of the fixed “sense” resistor, and V_{set} is the output of the digital to analog converter (DAC). When creating a positive supply, the DAC is given the two reference voltages V_{reg} and $V_{reg} - 5$ V, allowing the circuit to put out a current from 0 to 5 V/ R_s . For a negative supply, the desired range for V_{set} is from V_{reg} up to $V_{reg} + 5$ V, producing a current from 0 to -5 V/ R_s .

The appropriate range for the DAC can be selected by using the correct jumpers and installing the 7.5 k Ω resistor in either the R_p or R_n position, as shown in Fig. 1. For a negative supply the 11 and 28.7 k Ω resistors should swap places from the positive supply configuration shown in Fig. 1.

We changed two filtering capacitors on the DAC inputs from 10 to 100 nF to improve noise immunity. As with the original design, R_{pot} is omitted when controlling the driver digitally. When using R_{pot} to set the current with a potentiometer, the buffering op-amp, the DAC, and their associated

^{a)}Electronic mail: dallin_durfee@byu.edu.

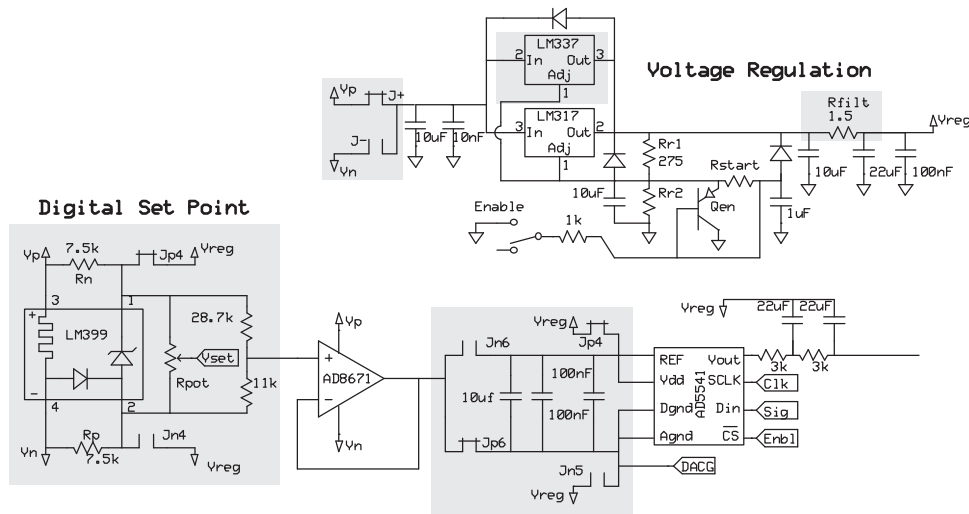


FIG. 1. The most significant changes to the driver are highlighted. As shown the schematic is configured for positive current.

passive components should be omitted. This configuration is simpler, but it degrades repeatability, noise, and drift.

We upgraded the digital and analog input/output cable to a DVI-I cable. This cable has 24 digital pins connected as twisted pairs as well as four shielded coaxial lines. The larger number of lines allows more devices to be wired in parallel and controlled by a single microcontroller. The shielded analog lines also reduce noise in the analog signal sent back to the microcontroller.

We rearranged the signal buffers for ease in laying out the PCB. The choice of op-amp for these buffers is not as critical as for many other components, but many op-amps were unable to drive the analog lines in a DVI-I cable without oscillating. We found that the TS514 op-amp is able to drive the lines, and many other chips would work as long as a 10 k resistor was put in series with the output.

An extra analog line was added which takes any 0 to 5 V signal from a BNC connector, buffers it with a differential amplifier, and sends it to the microcontroller in the same manner as the current monitor analog signal. This line can be used to digitally implement a laser stabilization technique such as the one discussed in Ref. 4, or for processing any other analog signal the user may desire.

In Ref. 1, current noise and drift were determined by measuring the voltage across a 2.5 Ω precision resistor in series with the output of the driver, as shown in Fig. 2(a). The voltage was measured with a Lecroy Waverunner LT 354 oscilloscope and Fluke 8505 multimeter. The measurement was limited by the measurement noise floor and therefore only represented an upper limit on the current driver noise and drift.

We recently used an improved setup involving both a positive and a negative current source, shown in Fig. 2(b). Each current driver was configured using lower current components and Vishay SMR3D precision resistors for R_s . One current driver was set to +50 mA and the other to -50 mA, such that almost all of the current flowed from one driver to the other through the two laser diodes. Uncorrelated current noise and drift induced a voltage across a 1 MΩ resistor. This

setup greatly reduced the bias in our noise/drift measurement and allowed us to use a larger resistor to increase the size of the signal. Unfortunately, the larger resistor also increased the time constant for our measurements, limiting us to measurements below a few kHz.

The results of our new measurements, as well as data from Ref. 1, are shown in Fig. 3. The noise spectrum in different frequency ranges was calculated from different datasets. The part of the spectrum below 2 Hz was calculated from a dataset taken using an 8505A digital multimeter, and the higher frequency ranges were calculated from several datasets taken using an LT 354 oscilloscope at different sample rates. For each dataset the signal was conditioned with an SR560 preamplifier configured with a 12 dB/octave low-pass filter. The preamplifier was set to unity gain and the filter cutoff frequency was set at least a factor of 20 below the sample rate of the multimeter or oscilloscope. After calculating the noise spectral density from each dataset, frequencies higher than one tenth of the filter cutoff frequency were considered invalid and thrown out.

The fact that the different data segments align seamlessly is an indication that significant aliasing or filter roll-off effects are not present. There are, however, discontinuities in the noise floor related to the intrinsic noise of the multimeter and the oscilloscope. The most notable jump is at 2 Hz where we switched from a dataset taken with the voltmeter to sets taken with the oscilloscope. Because the floor is well below

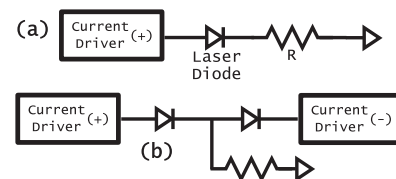


FIG. 2. Measurement layout. The measurement setup used in Ref. 1 is shown in the upper diagram (a). The lower diagram (b) is the improved setup used in this work.

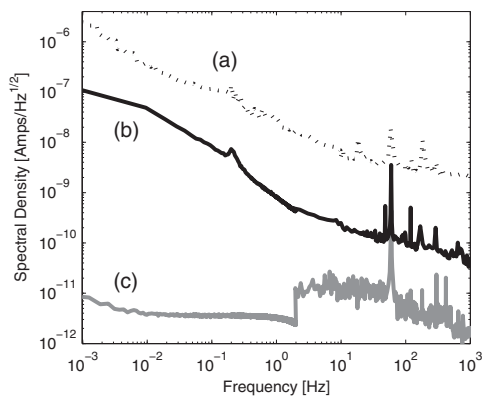


FIG. 3. Current noise spectral density. The data from Ref. 1 is shown as a dotted line (a). The new noise measurements are shown as a black line (b). The noise floor of the new measurement setup is shown as a gray line (c).

the measured noise, this does not significantly affect our measurement.

If we assume that the noise in the two current drivers is uncorrelated, the combined noise of the two drivers, N_{total} , is just a quadrature sum of the noise from each driver, N_1 and N_2 . If we further assume that both drivers produce similar

amounts of noise in any given band, then $N_{total} \approx \sqrt{2}N_1$. As such, the data presented in Fig. 3 represents the total measured noise from both drivers divided by $\sqrt{2}$.

Unlike the upper-limit measurement in Ref. 1, the new measurements are well above the noise floor, and therefore represent the actual noise and drift of the current driver. These measurements are about an order of magnitude below the noise floor of the previous measurement in Ref. 1.

In conclusion, we discussed modifications to a laser current driver which allow one PCB to be used to realize both positive and negative current supplies with a wide range of current capacity. We also presented improved noise and drift measurements which are significantly lower than all commercially available drivers we are aware of, and about an order of magnitude lower than our previously reported upper limit.

This work was funded by National Science Foundation (NSF) Award No. 0855490.

¹C. J. Erickson, M. Van Zjill, G. Doermann, and D. S. Durfee, *Rev. Sci. Instrum.* **79**, 073107 (2008).

²K. G. Libbrecht and J. L. Hall, *Rev. Sci. Instrum.* **64**, 2133 (1993).

³Annotated schematics and circuit board layout files can be downloaded at <http://www.physics.byu.edu/faculty/durfee/electronics.php>.

⁴S-w. Chiow, Q. Long, C. Vo, H. Müller, and S. Chu, *Appl. Opt.* **46**, 7997 (2007).